ORIGINAL RESEARCH ARTICLE

Keigairengyoto, a traditional Japanese medicine, promotes bacterial clearance by activating innate immune cells in mouse cutaneous infection models

Junichi Koseki[1], Atsushi Kaneko[1], Yosuke Matsubara[1], Kyoji Sekiguchi[1], Satomi Ebihara[1], Setsuya Aiba[2], Kenshi Yamasaki[2]*

[1] *Tsumura Research Laboratories, Tsumura & Co., Ibaraki, Japan*
[2] *Department of Dermatology, Tohoku University Graduate School of Medicine, Sendai, Miyagi, Japan*

ABSTRACT

Prompt elimination of pathogens including bacteria and dead cells prevents the expansion of secondary and prolonged inflammations and tissue damage. Keigairengyoto (KRT) is a traditional Japanese medicine prescribed for dermatoses such as purulent inflammations. Our aim is to clarify the actions of KRT in bacterial clearance and to examine the cell-kinetic profiles of phagocytes. In a mouse cutaneous infection model using living *Staphylococcus aureus*, KRT drastically reduced the number of bacteria in the infection sites. To evaluate the bacterial clearance, pseudo-infection was induced in mouse ears by intradermal injection of FITC-conjugated dead S. *aureus*. Biochemical and histological examinations revealed that KRT promoted bacterial clearance at 6 and 24 h post-injection. The numbers and phagocytic activities of neutrophils and macrophages in the ears were evaluated histologically using anti-Ly6G and F4/80 antibodies. KRT reduced bacterial deposition and increased the accumulation of F4/80$^+$ resident macrophages around the lesion site. FACS analysis was performed on single cell suspensions dispersed enzymatically from skin lesions, followed by an investigation of CD11b$^+$Ly6G$^+$ (neutrophils) and CD11b$^+$Ly6G$^-$ (monocytes/macrophages) cells. KRT increased the mean fluorescent intensity of FITC in CD11b$^+$Ly6G$^-$ cells and the number of FITC-positive CD11b$^+$Ly6G$^+$ cells, while KRT did not change the numbers of these cells. To investigate the active constituents of KRT, phagocytosis assay using macrophages was performed, resulting in that some flavonoid glucuronides of KRT derivatives augmented phagocytosis. Collectively, KRT promoted bacterial clearance by enhancing the phagocytic capability of neutrophils and macrophages. KRT may exert unique properties in preventive and therapeutic strategies for skin infectious inflammation.

Keywords: kampo; phagocytosis; resident macrophages; neutrophils; *Staphylococcus aureus*; flavonoid glucuronide; skin

*CORRESPONDING AUTHOR
Atsushi Kaneko, Tsumura Research Laboratories, Tsumura & Co., 3586 Yoshiwara, Ami-machi, Inashiki-gun, Ibaraki 300-1192, Japan; kaneko_atsushi@mail.tsumura.co.jp

Introduction

The skin functions as a barrier to pathogens such as bacteria. In injured skin or immunosuppressive conditions, bacteria can enter the body, leading to infectious inflammation. Chronic stimulation by bacteria can cause skin inflammation, and dysregulated responses to infection can induce life-threatening septic shock. Innate immune cells possess receptors for pathogen-associated molecular patterns (PAMPs) and eliminate foreign invaders[1]. Prompt, flexible, and appropriate clearance of PAMPs is important to prevent the expansion of excessive inflammatory reactions and prolonged inflammations.

Professional phagocytes, such as neutrophils, macrophages, and dendritic cells, play roles to eliminate harmful and/or inflammatory particles. Circulating neutrophils are rapidly recruited to infectious areas through chemotactic signals[2]. Neutrophils dominantly express various receptors for PAMPs and bear the primary defense against infection by killing bacteria through some bactericidal mechanisms[3]. Macrophages and dendritic cells are residents in the skin and function as sentinel cells in the body's first line of defense against microbes as well as neutrophils[4,5]. Macrophages have various types of receptors

for PAMPs and manage the innate immune system, while dendritic cells are the key cells in the development of acquired immune system as antigen-presenting cells. Macrophages have characteristics of diversity and plasticity in cell differentiation, therefore playing roles in inflammation and tissue repair and regeneration[6]. Resident dermal macrophages orchestrate the initiation and termination of immune response in skin infection[7]. A deficiency of macrophage function fails in the timely recruitment of neutrophils to the site of infection and delays bacterial clearance[7]. These lines indicate that resident dermal macrophages play important roles in the initial detection of skin-infiltrating bacteria and the activation of neutrophils.

Keigairengyoto (KRT) is a pharmaceutical grade traditional Japanese (*kampo*) medicine that is prescribed to patients with purulent dermatoses, which generate many dead neutrophils, followed by non-infectious inflammation. KRT is also prescribed to ameliorate purulent inflammation in other organs, such as empyema and rhinitis. KRT comprises 17 crude drugs and abundantly includes flavonoids, some of which enhance the phagocytic activity of myeloid leukemia cells and activate macrophage-like cells[8-12]. Genistein, which is rich in Glycyrrhizae radix, is reported to modify macrophage differentiation[13,14], inhibit LPS-induced downregulation of monocyte chemotactic protein-1(MCP-1) receptors, and promote the potentials of skin tissue repair[15-17]. Given that KRT is clinically effective against purulent inflammation in humans, these reports suggest that KRT enhances macrophage function. We therefore hypothesized that KRT activates innate immune response and promotes elimination of bacteria. As the skin resident bacterium *Staphylococcus aureus* is involved in skin diseases, such as impetigo and cellulitis, we evaluated the effects of KRT in mouse infection models using *S. aureus*. As expected, KRT markedly reduced the number of living *S. aureus* in the site of infection. We also examined the cell-kinetic profiles of neutrophils and macrophages in a pseudo-infection model using FITC-conjugated dead *S. aureus* and we observed KRT-enhanced bacterial clearance through modification of the immune system.

Materials and methods

Test drugs

KRT was supplied by Tsumura & Co. (Tokyo, Japan) in the form of a powdered extract. It was obtained by spray-drying a hot-water extract mixture of the following 17 crude drugs: Scutellariae radix,

Phellodendri cortex, Coptidisrhizoma, Platycodi radix, Aurantiifructusimmaturus, Schizonepetaespica, Bupleuri radix, Gardeniaefructus, Rehmanniae radix, Paeoniae radix, Cnidiirhizoma, Angelicae radix, Menthaeherba, Angelicaedahuricae radix, Saposhnikoviae radix, Forsythiaefructus, and Glycyrrhizae radix.

Many papers demonstrated that the commonly used and effective dose of *kampo* medicines is approximately 1 g/kg body weight in animal experiments including in dermatitis study[18,19]. Plasma pharmacokinetic study of bioactive flavonoids, which are speculated as active constituents of KRT, showed that they are absorbed promptly and transiently into the systemic circulation[18]. In order to examine the preventive effect of KRT, we administrated KRT at 0.25–2 g/kg body weight 1 h before and after cutaneous stimulation.

Prednisolone sodium succinate (PDN) was purchased from Shionogi Pharmaceutical Co. (Osaka, Japan) and used as a reference drug. Genistein 7-*O*-glucuronide and hesperetin 7-*O*-glucuronide were purchased from Toronto Research Chemical Industries (Toronto, ON, Canada). Liquiritigenin 4'-*O*-glucuronide, liquiritigenin 7-*O*-glucuronide, 18β-glycyrrhetinic acid, and cimifugin with purities high enough to be evaluated in biological tests were obtained from Analytical and Pharmaceutical Technology Research Center, Tsumura & Co. These compounds are absorbed through the digestive system and detected in the systemic circulation of humans and rats[18,20].

Animals

Male BALB/c and ICR mice were purchased from Japan SLC Inc. (Shizuoka, Japan) and Charles River Laboratories Japan Inc. (Kanagawa, Japan), respectively. Each mouse was used at 8–10 weeks old. This study was approved by and conducted according to the guidelines of the Experimental Animal Ethics Committees of Tsumura & Co.

Superficial skin infection model

Living S. aureus-induced cutaneous infection was performed in BALB/c mice according to the procedure described by Kugelberg *et al.* with a minor modification[21]. The hair on the back was shaved with an electric razor and depilatory cream under ketamine anesthesia was applied. An area of approximately 4 cm² was stripped with cloth-made cohesive tape once a day for two days. After the stripping in the second day, *S. aureus* MW2 (strain: BAA-1707, ATCC, Manassas, VA, USA)

was inoculated on the skin at 1×10^7 colony forming unit (CFU) in 100 μL saline. KRT was administrated orally to the mice at 1 and 2 g/kg in distilled water 1 h before and 1, 2, and 3 days after the inoculation. Skin lesion was examined at days 2 and 4 after the inoculation. The severities of erosion and papule were scored according to the following criteria: 0 (none), 1 (mild), 2 (moderate), and 3 (severe), and were indicated as the sum of each score. Mice were sacrificed by exsanguination under anesthesia at day 4 after the inoculation, and the skin of the infected site was excised and homogenized in saline. The homogenates were plated on staphylococcus agar to determine the number of living bacteria. The number of living bacteria was indicated as CFU per weight of the skin tissues (CFU/g).

Pseudo-infection model

Pseudo-infection model was performed in ICR mice using FITC-conjugated bioparticles of heat- or chemically-killed *S. aureus*, which were purchased from Thermo Fisher Scientific Inc. (Waltham, MA, USA). FITC-conjugated *S. aureus* (2×10^7 particles in 10 μL saline) or saline alone was intradermally injected into the ventral side of both ears using a microsyringe (Hamilton Co., Reno, NV, USA) under isoflurane anesthesia. KRT was administrated orally to the mice at 0.25 and 1 g/kg in distilled water 1 h before and 6 h after the injection. PDN was administrated orally to the mice at a dose of 10 mg/kg in distilled water. The mice were sacrificed by exsanguination under anesthesia 2, 6, or 24 h after the injection, and the ears were cut off for the following examinations.

Measurement of bacterial clearance

Bacterial clearance from the infected ears was evaluated by two methods. First, the ears were immersed in 1 N KOH and lysed completely, followed by the measurement of fluorescent intensity at an excitation wavelength of 495 nm and an emission wavelength of 528 nm. The amount of bacteria was calculated using a standard curve of serially diluted FITC-conjugated *S. aureus*. In the second method, the ears were stained by Gram's method as described in the next section, and the depositions of Gram-stained bacteria were semi-quantified by image analysis using BZ-X analyzer software (Keyence, Osaka, Japan).

Histological evaluation

The back skin and the ears were fixed with 10% formaldehyde and 4% paraformaldehyde, respectively. The fixed tissues were embedded in paraffin and cut into 4-μm cross-sections. The specimens were stained with hematoxylin and eosin (HE) or Gram-Hacker's solution. For immunofluorescent analysis, sections were stained using 2 μg/mL of anti-mouse F4/80 (clone: A3-1, Bio-Rad Laboratories Inc., Hercules, CA, USA) and 1 μg/mL of Alexa 647-conjugated anti-rat IgG2b (Thermo Fisher Scientific Inc.), or 2 μg/mL of biotin-conjugated anti-mouse Ly6G (clone: 1A8, BioLegend, San Diego, CA, USA) and 0.1 μg/mL of APC-conjugated streptavidin (BioLegend), and then mounted using ProLong Gold Antifade Reagent with DAPI (Thermo Fisher Scientific). All images were taken using a Biorevo BZ-X700 fluorescence microscope and BZ-X viewer software (Keyence). The accumulation of F4/80-positive cells in the inflamed ears was evaluated as the number of positive cells per unit area within the range of 200 μm around the clumps of bacteria and/or abscesses. F4/80-positive cells were identified according to the double-positive stain of Alexa647 and DAPI.

Measurement of chemokines and cytokines in inflamed ears

The ears obtained at 1 h after the *S. aureus* injection were frozen immediately in liquid nitrogen, and then were crushed using a cryopress machine (Microtec Co., Chiba, Japan). The crushed ears were homogenized in cold PBS supplemented with a cocktail of proteinase inhibitors (Sigma-Aldrich, St. Louis, MO, USA) and centrifuged at 10,000 g for 15 min at 4 °C. MCP-1, interleukin-1β (IL-1β), and keratinocyte chemoattractant (KC) in the supernatant of homogenates were quantified using ELISA kits according to the manufacturer's instructions (R&D Biosystems, Minneapolis, MN, USA). Total protein was measured by the Lowry assay (Thermo Fisher Science) using bovine serum albumin as a standard.

Immune cell analysis by flow cytometry

The procedure was performed according to the previous report with a minor modification[7]. The ear was cut into nine pieces, followed by enzymatic digestion in PBS containing 0.45 mg/mL dispase I (Roche Diagnostics, Indianapolis, IN, USA), 2 mg/mL collagenase II (Sigma-Aldrich), and 0.32 mg/mL DNase I (Sigma-Aldrich) for 2 h while shaking at 37 °C. Single-cell suspensions were prepared by mechanical disruption in ice-cold Dulbecco's Modified Eagle Medium (DMEM) supplemented with 10% FBS, followed by filtration through a 70-μm cell strainer. After centrifugation twice, the cells were gently suspended in 30% Percoll (GE Healthcare, Piscataway, NJ, USA),

and then centrifuged at 630 g for 20 min to isolate and remove sebum, low-density cells and debris. Cell pellets were re-suspended in 10% FBS DMEM and passed through a 40-μm cell strainer. After centrifugation, the cells were fixed with paraformaldehyde and stored at 4 °C until flow cytometric analysis. After blocking non-specific binding using mouse IgG1 (clone MG1-45, BioLegend), the following antibodies to mouse antigens were used: PE anti-mouse CD45 (clone: 30-F11, BD Bioscience, San Diego, CA, USA), PE/Cy7 anti-CD11b (clone: 30-F11, BioLegend), and biotin anti-Ly6G (clone: 1A8, BioLegend). APC-conjugated streptavidin was used for the secondary reagents. Cell samples were analyzed with a two-laser flow cytometer FACSaria II, and the data were analyzed with Diva software version 8.0.1 provided by Becton, Dickinson & Company (San Jose, CA, USA). Debris (FCS *vs.* SSC) and doublets (FSC-H *vs.* FSC-A) were excluded. Cells from the ears of a naive mouse showed approximately 15% CD45-positive and approximately 8% CD11b-positive cell populations in the whole cells. Phagocytic activity was shown as the mean fluorescence intensity (MFI) of whole cells.

Measurement of ear thickness

Ear thickness was measured using a dial thickness gauge micrometer (Ozaki MFG Co., Tokyo, Japan), at 0, 2, 6, and 24 h after the injection of FITC-conjugated *S. aureus* in mice under isoflurane anesthesia. All data on the increase in ear thickness were expressed as a percentage of the previous value in each individual mouse.

Macrophage culture assay

Cells of mouse macrophage cell line RAW264.7 (ATCC, Manassas, VA, USA) were grown in DMEM supplemented with 10% FBS, 4.5 g/L glucose, 2 mmol/L L-glutamine, 100 U/mL penicillin, 100 μg/mL streptomycin, and 10 mmol/L HEPES. Cells were seeded in 96-well culture plates at 5×10^3 cells/well, and cultured with the test compound (30 μmol/L) in the presence or absence of the suboptimal-dose 0.5 ng/mL mouse interferon-γ (IFN-γ) (PeproTech Inc., Rocky Hill, NJ, USA). After 3 days of incubation at 37 °C, culture fluids were removed and FITC-conjugated *S. aureus* at 30 μg/mL in warm medium was added. After 30-min incubation in a 5% CO_2 incubator, cells were harvested using cold PBS containing 2 mmol/L EDTA, then washed and treated for 15 min at 4 °C with phosphate buffer containing 4% paraformaldehyde (pH 7.4). FITC-positive cells were determined using a FACSaria II flow cytometer

and DIVA 8.0.1 software. Activity was indicated as the MFI of whole cells.

Definition of group names and statistical analysis

A mouse not treated with *S. aureus* was defined as "normal", and a mouse treated with *S. aureus* alone (no KRT) was defined as a "control". The 0.25, 1, and 2 g/kg of KRT were described as KRT-L, KRT-M, and KRT-H, respectively. All values are expressed as mean ± SEM. Student's *t*-test was performed to compare normal and control groups. Tukey's, Tukey–Kramer, Steel's, Steel–Dwass, and Dunnett's tests were used to perform multiple comparisons between groups, or between control groups and drug-administered groups. A probability of <0.05 was considered significant.

Results

KRT reduces the number of living *S. aureus* in the cutaneous infection

We first investigated the effects of KRT on superficial skin infection model. The number of living bacteria in control mice was 726.3 ± 155.6 ($\times 10^5$ CFU/g) at 4 days post the inoculation (**Figure 1A**). KRT-M (1 g/kg) and KRT-H (2 g/kg) dramatically reduced the number of living bacteria to 6.2 ± 0.4 and 3.5 ± 1.1 ($\times 10^5$ CFU/g), respectively. Macroscopic lesion scores at 2 and 4 days were lower in mice treated with KRT-M or KRT-H than the control mice (**Figure 1B**). Representative macroscopic images are shown in **Figure 1C**. An extensive erosion with severe crust formation was observed in the back skin of control mice at day 2. In contrast, those of the mice treated with KRT-M and KRT-H showed milder skin lesion with less erosion and crust formation, and erosions and papules were hardly observed in KRT-H-treated mice at day 4. Histological observation revealed that KRT suppressed acanthosis and spongiosis in epidermis and edema in dermis (**Figure 1D**).The quantitative analysis of histological observations results are shown in **Supplementary Figure S1**.

KRT augments clearance of *S. aureus*

In order to focus on action of bacterial clearance, we next examined the effects of KRT in pseudo-infection model using FITC-conjugated dead *S. aureus*. We first examined, on whether KRT accelerates bacterial clearance, by measuring the amount of remaining FITC-conjugated *S. aureus* in the ear (**Figure 2A**). The amount of bacteria in
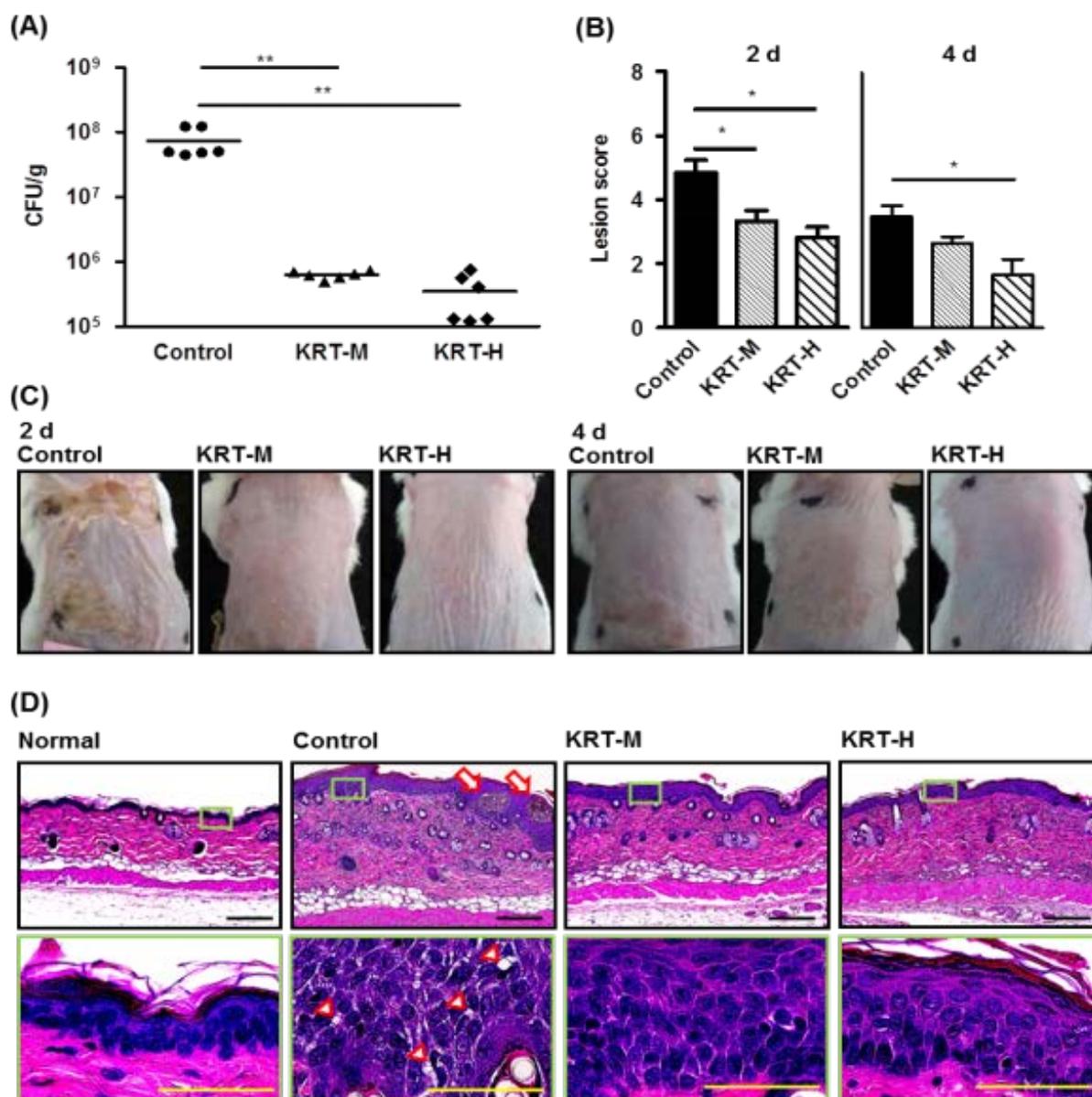
Figure 1. Keigairengyoto showed anti-microbial activities in a superficial skin infection model using living *Staphylococcus aureus*.
After tape stripping from the back skin of mice, *S. aureus* was inoculated at 1×10^7 CFU in $100\,\mu$L. Keigairengyoto (KRT, 1 and 2 g/kg) suspended in distilled water was administered orally to mice at 1 h before and 1, 2, and 3 days after the inoculation. The back skins were excised from mice on day 4. The number of living bacteria was measured on day 4 (**A**). Macroscopic damage scores of the infection sites were evaluated on day 2 and 4 (**B** and **C**). The skin sections on day 4 were stained with hematoxylin and eosin staining. Representative images are shown as low-power (upper panels) and high-power (lower panels); green boxes: the sites of each magnification; arrows: pustule; arrowheads: spongiosis; black bars: $200\,\mu$m; and yellow bars: $50\,\mu$m (**D**). $N = 2$ (normal) or 6 (control, KRT-M, and KRT-H). ******: $P < 0.01$; *****: $P < 0.05$ (Steel's test).

control mice was above 200 μg/ear at 2 h post-*S. aureus* injection and gradually decreased to less than half by 24 h. KRT-M significantly decreases the amount of bacteria at 6 and 24 h post-injection, though it shows no difference at 2 h. PDN exhibited no difference from the control at any time point. We histologically evaluated the bacterial clearance at 6 h post-injection in Gram-stained specimens. In control mice, gram-positive bacteria were deposited in the dermis of the ears (**Figure 2B**). KRT-M significantly decreased the deposition of gram-positive bacteria (**Figures 2B** and **2C**). In contrast, PDN exhibited no difference from control. These findings indicated that KRT promoted bacterial clearance.
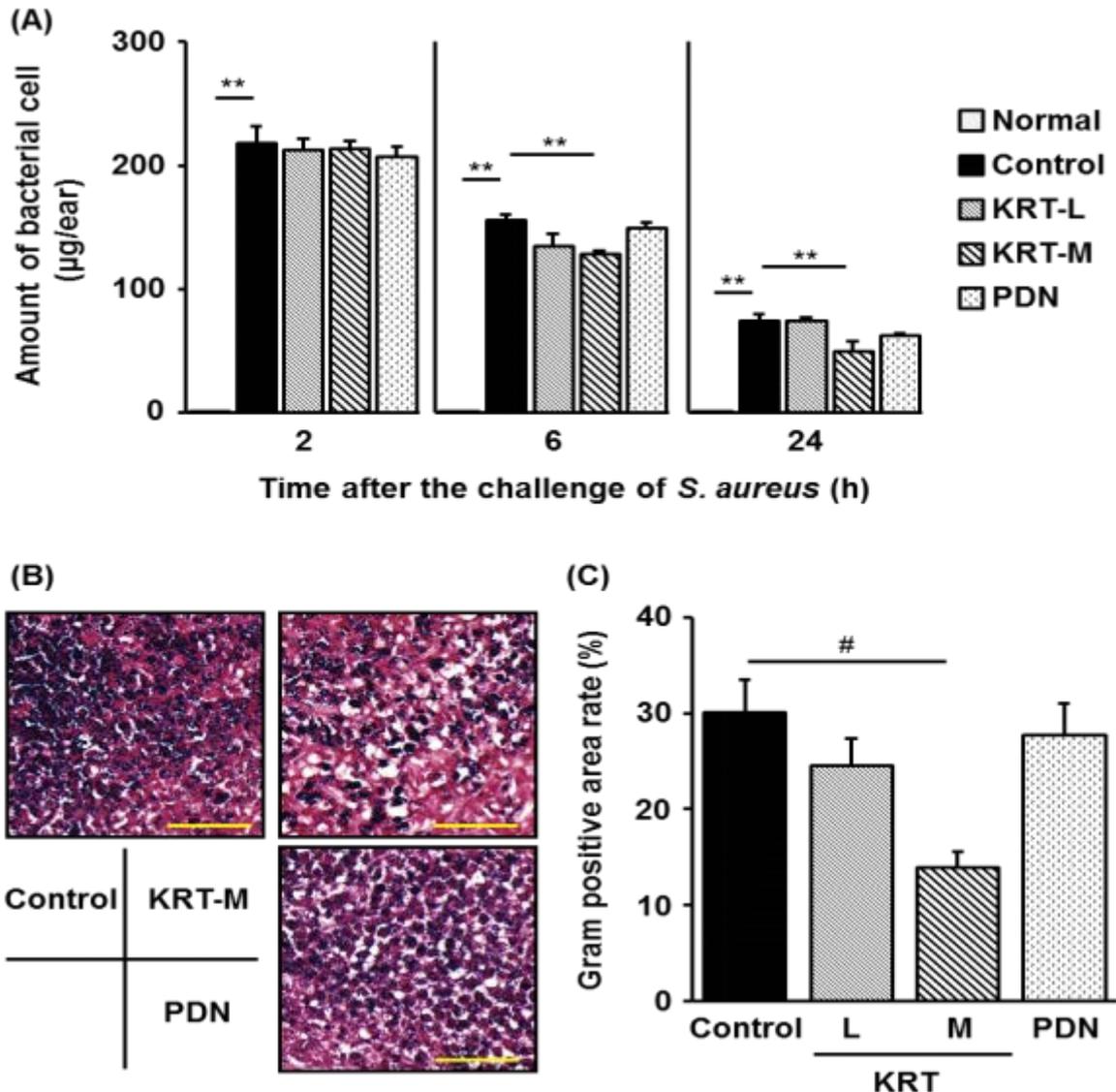
Figure 2. Enhancement of bacterial clearance by Keigairengyoto administration.
FITC-conjugated bioparticles of killed *S. aureus* were injected into both ears at 2×10^7 particles/10 μL/site. The ears were cut off at 2, 6, and 24 h after injection. Keigairengyoto (0.25 and 1 g/kg) suspended in distilled water or prednisolone (10 mg/kg) was administered orally to mice at 1 h before and 6 h after the injection. The amount of bacteria in the ears was measured biochemically at 2, 6, and 24 h after the injection (**A**). The ear sections were stained with Gram-Hacker's solution (**B**) and the deposition of Gram-positive bacteria in the lesion area was measured at 6 h after injection by an image-analysis technique (**C**). Yellow bars indicate 50 μm. $N = 8$. **: $P < 0.01$ (Tukey's test); #: $P < 0.05$ (Dunnett's test).

KRT reduces FITC-positive signals in clumps of *S. aureus*

Neutrophils were visualized as Ly6G⁺ cells by fluorescent staining, and the localization of Ly6G⁺ cells in clumps of FITC-conjugated bacteria was observed (**Figure 3**). In control mice, Ly6G⁺ cells (red fluorescence) infiltrated mildly around the clumps of bacteria (green fluorescence) at 2 h, the cell infiltration had increased at 6 h, and an abscess had formed in the dermis with a decrease in FITC-conjugated bacteria at 24 h. In KRT-M-treated mice at 6 h, Ly6G⁺ cells infiltrated more toward the center of bacteria clumps, which resulted in a pattern of dispersed FITC-positive signals at the periphery and compact highly FITC-positive signals in the center of the lesion. PDN-treated mice showed a similar distribution of Ly6G⁺ cells in FITC-conjugated bacteria compared with control mice. Semi-quantitative image analysis of Ly6G-positive signals in the
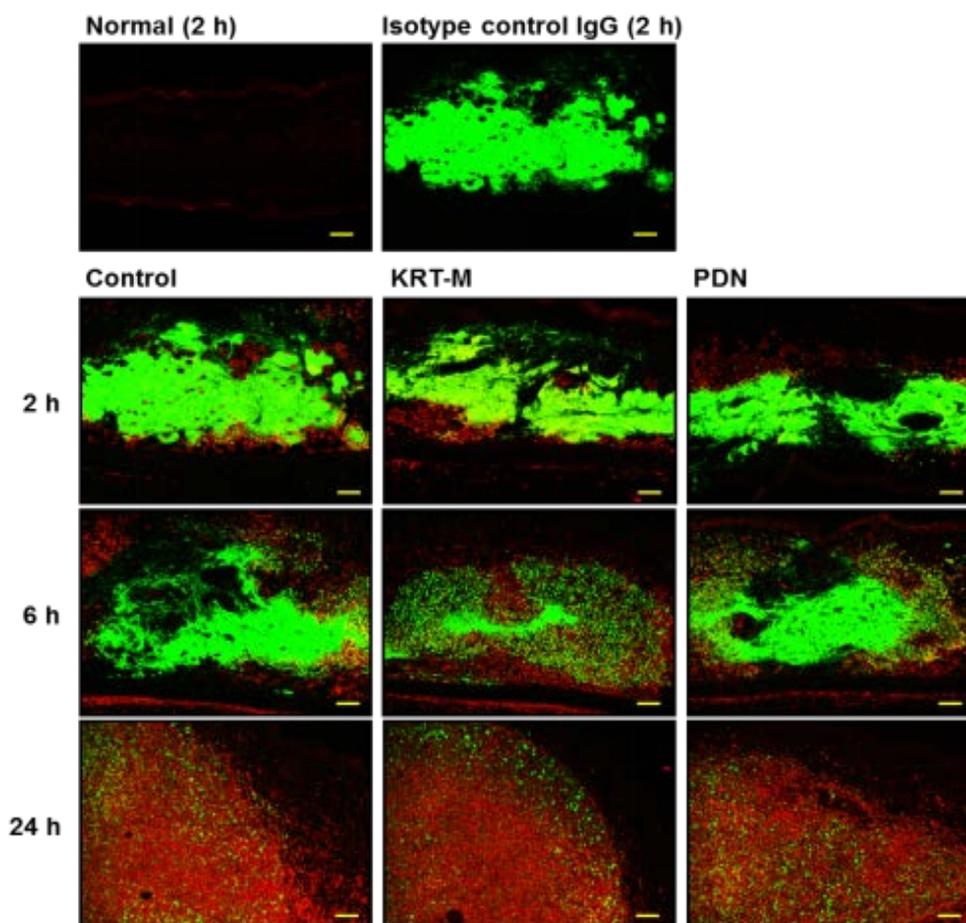
Figure 3. Keigairengyoto-induced enhancement of phagocytosis of Ly6G-positive cells.
The ears injected with FITC-conjugated *S. aureus* were cut off at 2, 6, and 24 h, and then subjected to immunofluorescence staining for Ly6G. Red and green indicate Ly6G-positive cells and FITC-conjugated *S. aureus*, respectively. Yellow bars indicate 50 μm.

lesions revealed no remarkable difference between groups at 6 h (data not shown). These results suggested that KRT treatment enhanced neutrophil penetration into the bacterial clumps at certain time periods, but did not significantly increase neutrophil numbers in the lesion.

KRT accelerates accumulation of macrophage-like cells around clump of *S. aureus*

HE-staining images at 6 h after the bacterial injection are shown in **Figure 4**. In normal mice without bacteria injection, resident macrophages—which had mononuclear morphology and larger cell size than resident lymphocytes—are observed. Macrophages-like cells, as well as polynucleated neutrophils, accumulated to the dermis around the bacteria clump in control mice at 6 h. In mice treated with KRT-M, the frequency of macrophages-like cells around the bacteria clumps was higher than control and showed larger abscesses at 6 h post-injection. Mice treated with PDN did not show a remarkable difference in macrophage-like cell infiltration compared with control mice.

KRT enhances F4/80⁺ cell accumulation to the lesion

To clarify the cell-type of macrophage-like cells observed in **Figure 4**, fluorescent staining using anti-F4/80 antibody was performed. F4/80 protein is expressed mainly in resident macrophages, while monocytes also express it at a lower level than macrophages. $F4/80^+$-resident macrophages were observed in the dermis of normal mice, as shown in **Figure 5A**. $F4/80^+$ cells were accumulated around the bacteria clumps in control mice at 2 h after the bacterial injection. Mice treated with KRT-M showed more accumulation of $F4/80^+$ cells compared with the control, and this was confirmed by counting the number of $F4/80^+$ cells per unit area around the lesion site (**Figure 5B**). PDN-treated mice showed
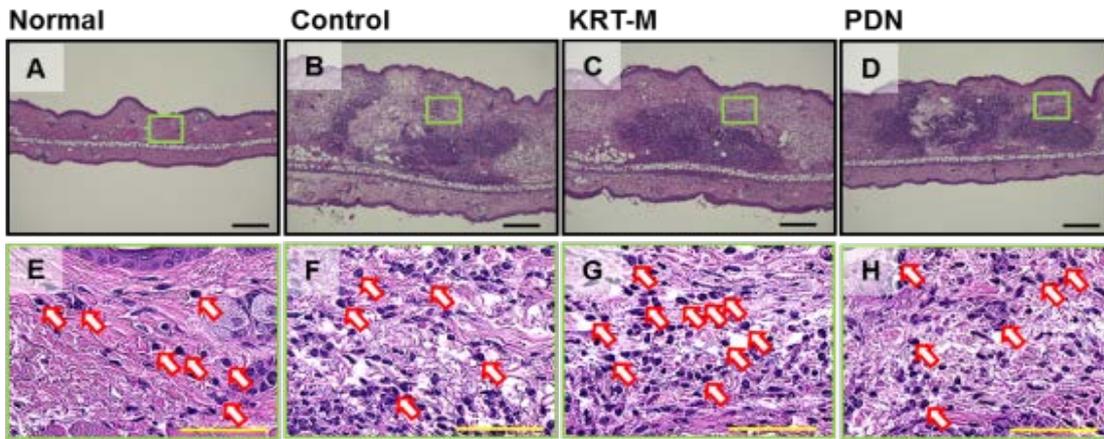
Figure 4. Histological analysis of cell kinetics by hematoxylin and eosin stain.
The ears were harvested at 6 h after the injection of FITC-conjugated *S. aureus* and evaluated histologically by hematoxylin and eosin staining. Representative images of low-power (upper panels) and high-power (lower panels) fields of the ear sections are shown for normal (**A** and **E**), control (**B** and **F**), KRT-H (**C** and **G**), and PDN (**D** and **H**). Green boxes indicate the sites of each magnification, and arrows indicate macrophage-like cells. Black and yellow bars indicate 200 and 50 μm, respectively.
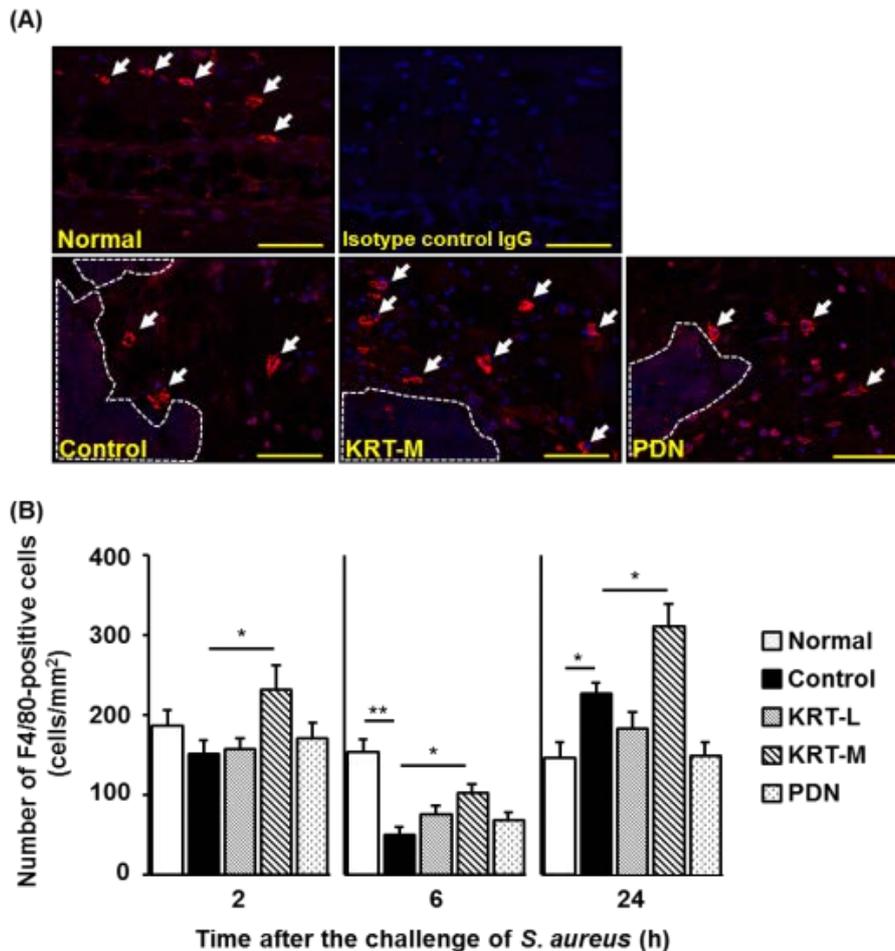

Figure 5. Keigairengyoto's effects on the accumulation of F4/80-positive cells at the lesion site.
(**A**) The ears injected with FITC-conjugated *S. aureus* were cut off 2, 6, and 24 h later and subjected to immunofluorescence staining for F4/80. Representative images of F4/80-positive cells are shown at 2 h after the injection. Arrows and areas surround by white dotted lines indicate F4/80-positive cells and clumps of bacteria, respectively. Yellow bars indicate 50 μm. (**B**) F4/80-positive cells were counted as the number of positive cells per unit area around the clump of bacteria or abscess in the ears at 2, 6, and 24 h after the injection. Yellow bars indicate 50 μm. $N = 7$ or 8. *: $P < 0.05$; **: $P < 0.01$ (Tukey-Kramer test).

levels of F4/80$^+$ cells similar to control mice at 2 and 6 h, but fewer F4/80$^+$ cells than control and KRT-M treated mice at 24 h. These results indicated that KRT-M increased the accumulation of F4/80$^+$ resident macrophages at the bacteria clumps.

Next, we investigated whether KRT affects the production of chemokines and cytokines related to macrophage functions. As KRT enhanced F4/80$^+$ cell accumulation compared to controls as early as 2 h, we examined the chemokine and cytokine production in the ears at 1 h after bacteria inoculation. KRT-M, however, showed no difference in the production of KC, MCP-1, and IL-1β at 1 h after the injection (**Figure 6**). We also measured them at 6 h post-injection and observed that KRT treatment did not alter the expression of these chemokines in the lesion (data not shown).

KRT augments phagocytosis by infiltrated cells *in vivo*

To quantitate numbers, populations, and phagocytic activity of macrophages and neutrophils in the lesions, FACS analysis was performed at 6 h after the *S. aureus* inoculation. In this study, CD11b$^+$Ly6G$^-$ and CD11b$^+$Ly6G$^+$ cells were designated as monocyte/macrophages and neutrophils, respectively. There was no change in the number of CD11b$^+$Ly6G$^-$ cells among the groups of normal, control, and KRT-treated mice. In

contrast, the number of CD11b$^+$Ly6G$^+$ cells had clearly increased in the control group at 6 h after the injection compared to the normal group, but the difference between control and KRT-M-treated groups was not significant (**Table 1**). The number of FITC-positive CD11b$^+$Ly6G$^+$ cells, which were *S. aureus*-ingesting neutrophils, significantly increased in the KRT-M-treated group compared with the control group. Moreover, the MFIs of FITC in both CD11b$^+$Ly6G$^-$ and FITC-positive CD11b$^+$Ly6G$^-$ cells were significantly increased in the KRT-M-treated group. These findings indicated an adjuvant effect of KRT on the phagocytic response to a foreign pathogen. Representative blots are shown in **Supplementary Figure S2**.

KRT suppresses ear swelling due to *S. aureus* inoculation

It generally is thought that the activation of innate immune cells may exacerbate inflammatory symptoms. Therefore, we examined the effect of KRT on ear thickness (**Figure 7**). At 2, 6, and 24 h after the injection, the ear thickness of control mice had increased 1.7, 2.4, and 2.9 times compared with that of normal mice, respectively. We did not observe remarkable differences in ear swelling between control and KRT-M at 2 h after bacteria inoculation or abscess formation (**Supplementary Figure S3**). Of note, KRT-M significantly suppressed the
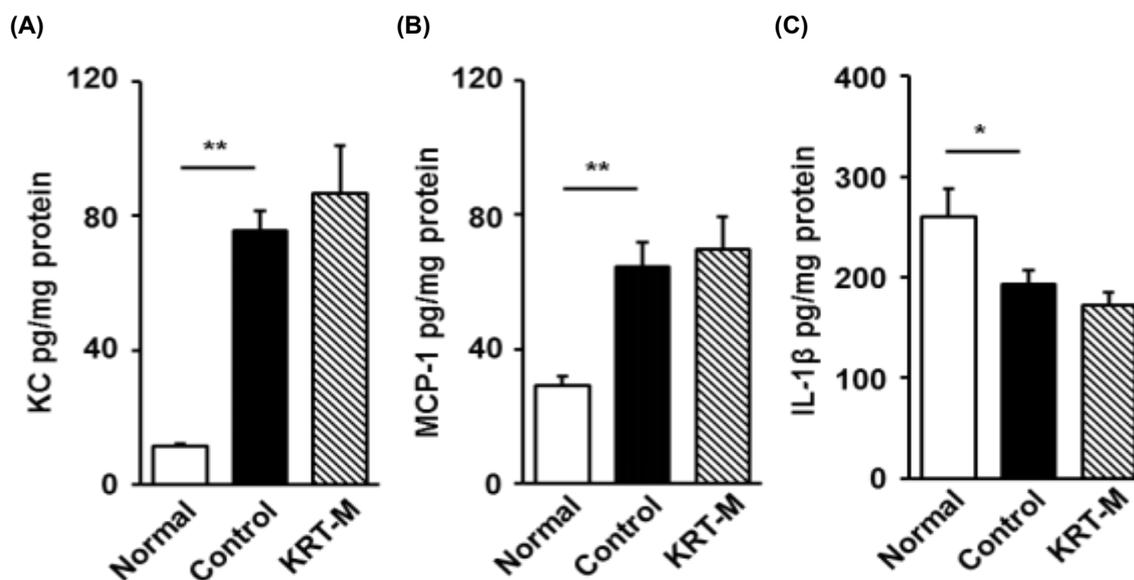

Figure 6.   Keigairengyoto's effects on the production of chemokines and cytokines.
Keigairengyoto (KRT-M, 1.0 g/kg) suspended in distilled water was administrated orally to mice at 1 h before induction of dermatitis by intradermal injection of FITC-conjugated *S. aureus* into the ears at 2×10^7 particles/10 μL/site. The ears were cut off 1 h after the injection. KC (**A**), MCP-1 (**B**), or IL-1β (**C**) in homogenizations of the ears was quantified by their specific ELISA. *N* = 7 or 8. *: *P* < 0.05; **: *P* < 0.01 (Tukey-Kramer test).

Table 1. Cytometric analysis of phagocytes in ears of mice treated with Keigairengyoto

	Region	Cell number (×10⁴ cells per ear)			MFI of FITC	
		Normal	Control	KRT	Control	KRT
Monocytes/macrophages						
CD11b⁺Ly6G⁻ (whole)	R1	27.2	29.0±2.8	28.8±1.8	113±16	190±29*
CD11b⁺Ly6G⁻ FITC⁺	R3	-	5.8±0.9	7.4±1.1	484±39	673±55*
Neutrophils						
CD11b⁺Ly6G⁺ (whole)	R2	0.4	60.8±7.1	75.2±4.7	3,258±531	3702±374
CD11b⁺Ly6G⁺ FITC⁺	R4	-	36.1±4.7	53.5±5.2*	5,247±589	5226±420

Keigairengyoto suspended in water was given orally to mice at a dose of 1 g/10 mL/kg, and 1 h later, FITC-conjugated *S. aureus* was injected to the ears. The ears were removed 6 h post-injection, and single cells were prepared by an enzyme-dispersing procedure. Phagocytic cells in the single ear cells were stained by anti-mouse Ly6G and anti-mouse CD11b and analyzed by flow cytometry. Data are shown as mean of 2 (Normal), 6 (Control), and 6 (KRT) ears per a group. Total numbers of harvested ear cells were 293, 322±18, 354±11×10⁴, respectively. R1, R2, R3, and R4 indicate each region built in the dot plots of **Supplementary Figure S1**. There was no difference among groups. *: $P < 0.05$ significant with the Student's *t*-test.
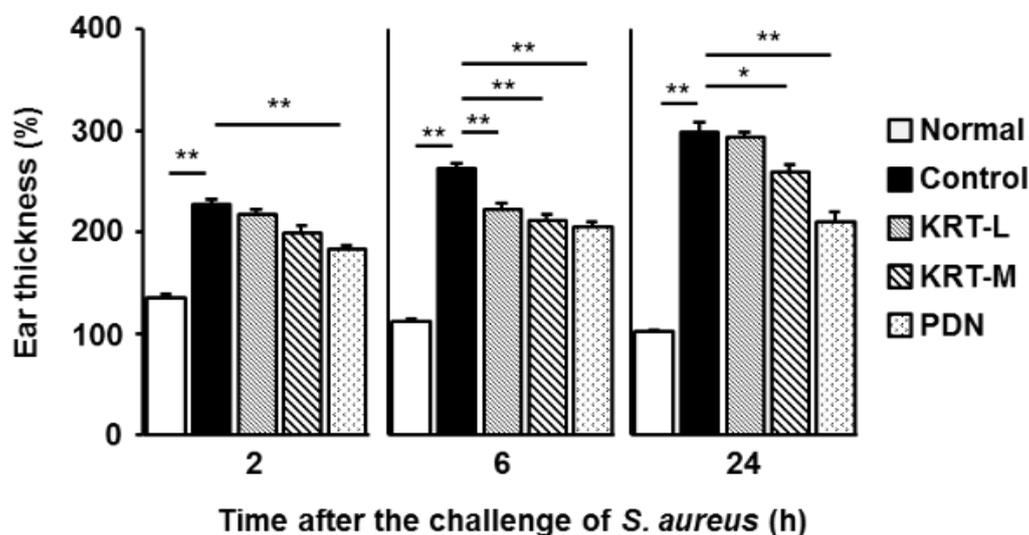
Figure 7. Suppression of ear thickness by Keigairengyoto administration.
Dermatitis was induced by intradermal injection of FITC-conjugated *S. aureus* into the ears. Ear thickness was measured at 0, 2, 6, and 24 h after injection. $N = 8$. *: $P < 0.05$; **: $P < 0.01$ (Steel-Dwass test).

increase in ear thickness at 6 h, though mice treated with KRT-M showed larger abscesses at 6 h post-injection, as shown in **Figure 4**. At 24 h, mice treated with KRT-M showed significantly thinner ears and smaller abscesses than control mice (**Supplementary Figure S3**). PDN also significantly suppressed ear swelling as well as abscess formation by *S. aureus* inoculation at all time points.

Active compounds of KRT augment phagocytosis by macrophages *in vitro*

Finally, we examined whether absorbed compounds related to KRT can augment macrophage functions *in vitro*. As shown in **Table 2**, genistein 7-*O*-glucuronide remarkably enhanced phagocytic activity in the macrophage cell line RAW264.7. Liquiritigenin 7-*O*-glucuronide also promoted phagocytosis by RAW264.7, while liquiritigenin 4'-*O*-glucuronide, hesperetin 7-*O*-glucuronide, 18β-glycyrrhetinic acid, and cimifugin were inactive in the present test.

Discussion

In this study, we demonstrated that KRT decreased the number of living bacteria and suppressed the development of the bacteria-induced skin lesions (**Figure 1**). Furthermore, we observed in the pseudo-infection model that KRT significantly decreased the numbers of dead bacteria at 6 and 24 h post-injection by measuring FTTC-signals in the homogenizations of the inflamed ears (**Figure 2A**). As a complementary test, the histological examination by Gram-

Table 2. Effects of Keigairengyoto-related compounds on macrophage phagocytosis

Test Sample	IFN-γ	Phagocytosis (MFI)
No IFN-γ	-	116±1
Control	+	134±2
Genistein 7-*O*-glucuronide	+	457±22**
Liquiritigenin 7-*O*-glucuronide	+	181±12*
Liquiritigenin 4'-*O*-glucuronide	+	139±3
Hesperetin 7-*O*-glucuronide	+	127±1
18β-glycyrrhetinic acid	+	143±4
Cimifugin	+	135±2

Mouse macrophage-like RAW264.7 cells were seeded in 96-well culture plates at 5×10^3 cells/well and cultured with test samples (30 μmol/L) in the presence or absence of suboptimal dose of 0.5 ng/mL mouse interferon-γ (IFN-γ). The culture fluids were removed after 3 days of culture and replaced with fresh medium containing FITC-conjugated *S. aureus* (30 μg/mL), followed by an additional culture for 0.5 h. The cells were harvested, and the FITC-positive cells were measured by FACSaria II. $N = 3$. *, **: $P < 0.05, 0.01$ *vs.* IFN-γ alone control (Dunnett's test), respectively.

stain indicated that KRT reduced *S. aureus* per unit lesion area 6 h after the injection (**Figure 2B**). Taken together, it is plausible to conclude that KRT enhances *S. aureus* clearance from infectious sites.

KRT is reported to have an anti-bacterial activity against *S. aureus* and *Propionibacterium acnes* in *in vitro* assays[22,23]. Therefore, the result of KRT in the infection model using living *S. aureus* may be due to direct attack against to the *S. aureus*. On the other hand, pseudo-infection experiment was performed in order to eliminate a possibility of direct bactericidal effect of KRT. It is plausible to conclude that KRT enhances the potentials of phagocytic cells, such as macrophage and neutrophils, and promotes bacterial clearance. It is unclear how much the enhancing effect of KRT on innate immune cells contributes to reducing the number of living *S. aureus* in the infection model. However, the enhancing effect of KRT is surely involved at least partially in bacterial clearance in the present infection model. One of the important strategies is to investigate a mechanism by which the bioactive flavonoids shown in **Table 2** enhance macrophage functions. We should examine cell-based kinetic study focusing on innate immune cells in the superficial skin infection model to clarify the effect of KRT, as well as the bioactive flavonoids, in more detail.

The histological examinations by HE and immunostaining using anti-F4/80 antibody indicated that KRT augmented resident macrophages accumulation around the clumps of bacteria or lesion site. Interestingly, KRT did not increase the number of CD11b$^+$Ly6G$^-$ cells in FACS analysis, which represented the number of macrophages per ear at 6 h post-injection (**Table 1**). Expression of F4/80 is heterogeneous and is modulated during macrophage maturation and activation. Monocytes that circulate in the bloodstream also express F4/80 on the surface, but the level is lower than that on resident macrophages. Langerhans cells and a subpopulation of dendritic cells also express F4/80. Since Langerhans cells reside mostly in the epidermis, dermal F4/80$^+$ cells measured in our study were mainly resident macrophages but not Langerhans cells. As the dermal resident macrophages are high in F4/80$^+$ and both resident macrophages and circulating macrophages are CD11b$^+$Ly6G$^-$, the accumulation of F4/80$^+$ macrophages around the bacteria clump is supposed to depend on the migration of resident macrophages from the nearby skin but not from the systemic circulation. Moreover, KRT increased phagocytosis by macrophages, which was shown as a higher MFI of FITC conjugated to *S. aureus* in CD11b$^+$Ly6G$^-$ cells than that of control group at 6 h in FACS analysis. FACS analysis performed at 2 h post-injection as well as the 6 h protocols similarly showed that KRT enhanced macrophage functions (data not shown).

Interestingly, our study found that the numbers of F4/80$^+$ cells per area around the lesion site in control groups decreased transiently at 6 h after the bacterial injection and then increased at 24 h, compared with normal groups. It is reported that *S. aureus* infection induces pyroptosis of resident macrophages, which is a pro-inflammatory programed cell death[24]. Macrophages that died by pyroptosis release alarmins including IL-1β, which induces recruitment and activation of neutrophils[25]. Cell death by pyroptosis is considered to play a crucial role for efficient elimination of bacteria. In an animal model of *S. aureus* skin infection, F4/80^{high} dermal macrophages initially decrease post-infection and expand later due to renewal by incoming Ly6C^{high} inflammatory monocytes[7]. Thus, our finding of the transient decrease of F4/80$^+$ cells may relate to the

characteristic modulation of F4/80-expressing cells during macrophage maturation and activation.

Neutrophils, represented as CD11b$^+$Ly6G$^+$ cells by FACS analysis, increased after inoculation with FITC-conjugated dead *S. aureus* (**Supplementary Figure S2**). Although KRT treatment did not increase the number of CD11b$^+$Ly6G$^+$ cells in the whole ears compared to the control, FITC-positive CD11b$^+$Ly6G$^+$ cells were significantly more numerous in KRT-treated mice than in the control (**Table 1**). The MFI of FITC in CD11b$^+$Ly6G$^+$ cells, which is a parameter of phagocytic potential per cell, was much higher than that in CD11b$^+$Ly6G$^-$ cells. Accordingly, Ly6G$^+$ cells were observed more frequently in the clump of FITC-positive *S. aureus* in the KRT-treated group at 6 h post-injection, and the histological images of FITC-positive *S. aureus* clumps were evidently fewer in KRT-treated group than that of control group (**Figure 3**). Circulating neutrophils are recruited rapidly to infectious areas through chemotactic signals and eliminate bacteria by bactericidal and phagocytic mechanisms[2,3,26]. Depletion of neutrophils delays bacterial clearance and causes lethality in mouse lung infection[27]. Considering that neutrophils are the most professional effect or cells against foreign pathogens, the capacity of KRT to promote bactericidal functions of neutrophils should be noted.

Some *kampo* medicines including KRT are flavonoid-rich. To evaluate the effects of KRT on phagocytosis by macrophage, we investigated the absorbed flavonoid compounds, which would be detected in the blood of mice that were given KRT orally. We recently demonstrated that jumihaidokuto, another *kampo* medicine that contains the same flavonoid-rich components as KRT, suppresses *Propionibacterium acne*-induced dermatitis by modulating macrophage function[19]. Considering our pharmacological and blood pharmacokinetic studies of jumihaidokuto[18,19], genistein 7-*O*-glucuronide, liquiritigenin 7-*O*-glucuronide, liquiritigenin 4'-*O*-glucuronide, hesperetin 7-*O*-glucuronide, 18β-glycyrrhetinic acid, and cimifugin were chosen for *in vitro* assays of macrophage phagocytosis in this study. Among these compounds, genistein 7-*O*-glucuronide was the most active in enhancement of phagocytosis. We recently clarified that glucuronides of phytoestrogen flavonoids, such as genistein and liquiritigenin, enhance macrophage functions *via* de-conjugation and stimulation of nuclear estrogen receptor in macrophages, resulting in the up-regulation of phagocytosis and expressions of complement receptors, Fc-receptors, chemotactic receptor, and so on[28]. Flavonoids of KRT would work directly on the innate immune system *in vivo*.

Proinflammatory cytokines and toxic radicals produced by activated macrophages would induce inflammatory symptoms such as edema and reddening of the skin. We measured ear thickness as a general clinical marker of skin inflammation after dead bacteria inoculation. To our surprise, although KRT recruited more macrophages and neutrophils to the bacteria clumps, KRT rather suppressed ear thickness at 6 and 24 h post-injection compared to the control. Histological observation in the infection model of living bacteria revealed that KRT suppressed edema of the epidermis and dermis in the lesion skin (**Figure 1D**). We observed that skin lesions of the KRT-treated group did not show obvious differences in KC, MCP-1 and IL-1β expression compared to the control group at 1 h post-injection (**Figure 6**). IL-1β was also measured at 6 h after the injection, but no difference was observed in KRT-treated mice (data not shown). These indicated that inhibitory effect of KRT on ear thickness did not depend on the modulation of proinflammatory cytokines induction.

KRT-treated mice showed thinner ears at 6 h while the bacteria had not been completely phagocytized and cleared. KRT-treated mice also showed less ear thickness and clearly smaller abscesses than the control at 24 h, suggesting that KRT enhanced the bacteria clearance at this point. PDN, which has strong inhibitory effects on various inflammatory responses, also suppressed ear thickness without affecting bacteria clearance. Therefore, KRT may have mechanisms other than promoting macrophage functions to suppress skin inflammation. In bacteria-infected sites, damaged cells, dead cells, and phagocytes produce toxic radicals. An excessive production of toxic radicals in the extracellular space can damage the surrounding healthy tissues and cause secondary non-infectious inflammation[29,30]. KRT has many blood-absorbing anti-oxidant constituents[31,32]. Our previous study demonstrated that liquiritigenin 7-*O*-glucuronide emerged in blood immediately after oral administration and exerted anti-oxidant activity[18]. Blood pharmacokinetic studies of active compounds originating from KRT could uncover the detailed mechanisms by which KRT exerts anti-inflammatory functions.

Conclusion

This is the first report to confirm that oral administration of KRT promoted bacteria clearance in mice. KRT activated resident macrophages to migrate to the bacteria lumps and promoted

phagocytosis against FITC-conjugated *S. aureus*. *In vitro* assays showed that absorbed flavonoids such as genistein 7-*O*-glucuronide remarkably promoted phagocytic activity in a macrophage cell line. Moreover, KRT enhanced the number of FITC-positive neutrophils in the ears, probably through the activation of resident macrophages (**Figure 8**). Thus, KRT activated the innate immune system, which was supported by the results in the infectious and pathophysiological model of the living bacteria.

Authors' contributions

J Koseki and A Kaneko performed experiments, analyzed data, prepared figures and tables, interpreted results of experiments, and drafted the manuscript. Y Matsubara, K Sekiguchi, and S Ebihara performed experiments and analyzed data. S Aiba interpreted results of experiments. K Yamasaki interpreted results of experiments and revised the manuscript. All authors reviewed and edited the manuscript, and approved the final version of the manuscript.

Acknowledgments

Appendix

The present manuscript contains three supplementary figures.

Conflict of interest

Dr. Kenshi Yamasaki and Dr. Setsuya Aiba received research grant support from Tsumura & Co. Junichi Koseki, Atsushi Kaneko, Kyoji Sekiguchi, Yosuke Matsubara, and Satomi Ebihara are employed by Tsumura & Co.

References

1. Tang D, Kang R, Coyne CB*, et al.* PAMPs and DAMPs: Signal 0s that spur autophagy and immunity. Immunol Rev 2012; 249(1): 158–175. doi: 10.1111/j.1600-065X.2012.01146.x.

2. McGuinness WA, Kobayashi SD, DeLeo FR. Evasion of neutrophil killing by *Staphylococcus aureus*. Pathogens 2016; 5(1). doi: 10.3390/pathogens5010032.

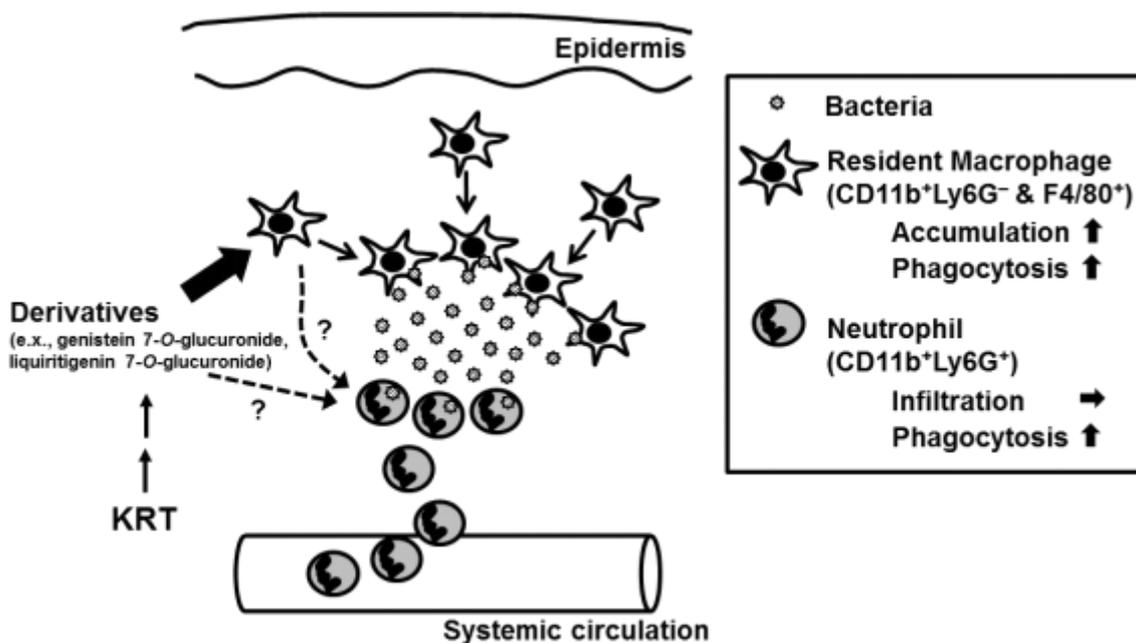3. Thomer L, Schneewind O, Missiakas D. Pathogenesis of *Staphylococcus aureus* bloodstream

Figure 8. Schema of possible action of KRT on bacterial clearance.
KRT enhances the functions of innate immune cells to accelerate the accumulation of resident macrophages (CD11b$^+$Ly6G$^-$ and F4/80$^+$) around bacteria clumps and bacterial phagocytosis by macrophages and neutrophils (CD11b$^+$Ly6G$^+$). KRT derivatives, such as genistein 7-*O*-glucuronide and liquiritigenin 7-*O*-glucuronide, may activate resident macrophages directly and augment host innate immune functions.

infections. Annu Rev Pathol 2016; 11: 343–364. doi: 10.1146/annurev-pathol-012615-044351.

4. Tay SS, Roediger B, Tong PL*, et al.* The skin-resident immune network. Curr Dermatol Rep 2014; 3: 13–22. doi: 10.1007/s13671-013-0063-9.

5. Malissen B, Tamoutounour S, Henri S. The origins and functions of dendritic cells and macrophages in the skin. Nat Rev Immunol 2014; 14(6): 417–428. doi: 10.1038/nri3683.

6. Ferrante CJ, Leibovich SJ. Regulation of macrophage polarization and wound healing. Adv Wound Care (New Rochelle) 2012; 1(1): 10–16. doi: 10.1089/wound.2011.0307.

7. Feuerstein R, Seidl M, Prinz M*, et al.* MyD88 in macrophages is critical for abscess resolution in staphylococcal skin infection. J Immunol 2015; 194(6): 2735–2745. doi: 10.4049/jimmunol.1402566.

8. Kawaii S, Tomono Y, Katase E*, et al.* Effect of citrus flavonoids on HL-60 cell differentiation. Anticancer Res 1999; 19(2A): 1261–1269.

9. Fung MC, Szeto YY, Leung KN*, et al.* Effects of biochanin A on the growth and differentiation of myeloid leukemia WEHI-3B (JCS) cells. Life Sci 1997; 61(2): 105–115. doi: 10.1016/S0024-3205(97)00365-2.

10. Yamazaki S, Morita T, Endo H*, et al.* Isoliquiritigenin suppresses pulmonary metastasis of mouse renal cell carcinoma. Cancer Lett 2002; 183(1): 23–30. doi: 10.1016/S0304-3835(02)00113-1.

11. Lim EK, Mitchell PJ, Brown N*, et al.* Regio-specific methylation of a dietary flavonoid scaffold selectively enhances IL-1beta production following Toll-like receptor 2 stimulation in THP-1 monocytes. J Biol Chem 2013; 288(29): 21126–21135. doi: 10.1074/jbc.M113.453514.

12. Lee J, Kim SL, Lee S*, et al.* Immunostimulating activity of maysin isolated from corn silk in murine RAW 264.7 macrophages. BMB Rep 2014; 47(7): 382–387. doi: 10.5483/BMBRep.2014.47.7.191.

13. Takahashi T, Kobori M, Shinmoto H*, et al.* Structure-activity relationships of flavonoids and the induction of granulocytic- or monocytic-differentiation in HL60 human myeloid leukemia cells. Biosci Biotechnol Biochem 1998; 62(11): 2199–2204. doi: 10.1271/bbb.62.2199.

14. Lee SH, Kim JK, Jang HD. Genistein inhibits osteoclastic differentiation of RAW 264.7 cells *via* regulation of ROS production and scavenging. Int J Mol Sci 2014; 15(6): 10605–10621. doi: 10.3390/ijms150610605.

15. Xu L, Khandaker MH, Barlic J*, et al.* Identification of a novel mechanism for endotoxin-mediated down-modulation of CC chemokine receptor expression. Eur J Immunol 2000; 30(1): 227–235. doi: 10.1002/1521-4141(200001)30:1<227::AID-IMMU227>3.0.CO;2-X.

16. Park E, Lee SM, Jung IK*, et al.* Effects of genistein on early-stage cutaneous wound healing. Biochem Biophys Res Commun 2011; 410(3): 514–519. doi: 10.1016/j.bbrc.2011.06.013.

17. Emmerson E, Campbell L, Ashcroft GS*, et al.* The phytoestrogen genistein promotes wound healing by multiple independent mechanisms. Mol Cell Endocrinol 2010; 321(2): 184–193. doi: 10.1016/j.mce.2010.02.026.

18. Matsumoto T, Matsubara Y, Mizuhara Y*, et al.* Plasma pharmacokinetics of polyphenols in a traditional Japanese medicine, jumihaidokuto, which suppresses *Propionibacterium acnes*-induced dermatitis in rats. Molecules 2015; 20(10): 18031–18046. doi: 10.3390/molecules201018031.

19. Sekiguchi K, Koseki J, Tsuchiya K*, et al.* Suppression of *Propionibacterium acnes*-induced dermatitis by a traditional Japanese medicine, jumihaidokuto, modifying macrophage functions. Evid Based Complement Alternat Med 2015; 2015: 439258. doi: 10.1155/2015/439258.

20. Asl MN, Hosseinzadeh H. Review of pharmacological effects of *Glycyrrhiza sp*. and its bioactive compounds. Phytother Res 2008; 22(6): 709–724. doi: 10.1002/ptr.2362.

21. Kugelberg E, Norstrom T, Petersen TK*, et al.* Establishment of a superficial skin infection model in mice by using *Staphylococcus aureus* and *Streptococcus pyogenes*. Antimicrob Agents Chemother 2005; 49(8): 3435–3441. doi: 10.1128/AAC.49.8.3435-3441.2005.

22. Higaki S, Hasegawa Y, Morohashi M*, et al.* The correlation of Kampo formulations and their ingredients on anti-bacterial activities against *Propionibacterium acnes*. J Dermatol 1995; 22(1): 4–9. doi: 10.1111/j.1346-8138.1995.tb03332.x.

23. Higaki S, Morimatsu S, Morohashi M*, et al.* Susceptibility of *Propionibacterium acnes*, *Staphylococcus aureus* and *Staphylococcus epidermidis* to 10 Kampo formulations. J Internat Med Res 1997; 25(6): 318–324. doi: 10.1177/030006059702500602.

24. Accarias S, Lugo-Villarino G, Foucras G*, et al.* Pyroptosis of resident macrophages differentially orchestrates inflammatory responses to *Staphylococcus aureus* in resistant and susceptible mice. Eur J Immunol 2015; 45(3): 794–806. doi: 10.1002/eji.201445098.

25. LaRock CN, Cookson BT. Burning down the house: Cellular actions during pyroptosis. PLoS Pathog 2013; 9(12): e1003793. doi: 10.1371/journal.ppat.1003793.

26. Koller W, Vetere-Overfield B, Gray C*, et al.* Failure of fixed-dose, fixed muscle injection of botulinum toxin in torticollis. Clin Neuropharmacol 1990; 13(4): 355–358. doi: 10.1097/00002826-199008000-00011.

27. Robertson CM, Perrone EE, McConnell KW*, et al.* Neutrophil depletion causes a fatal defect in murine pulmonary *Staphylococcus aureus* clearance. J Surg Res 2008; 150(2): 278–285. doi: 10.1016/j.jss.2008.02.009.

28. Kaneko A, Matsumoto T, Matsubara Y*, et al.* Glucuronides of phytoestrogen flavonoid enhance macrophage function *via* conversion to aglycones by β-glucuronidase in macrophages. Immun Inflamm Dis 2017. In Press. doi: 10.1002/iid3.163.

29. Flannagan RS, Heit B, Heinrichs DE. Anti-microbial mechanisms of macrophages and the immune evasion strategies of *Staphylococcus aureus*. Pathogens 2015; 4(4): 826–868. doi: 10.33 90/pathogens4040826.

30. Rigby KM, DeLeo FR. Neutrophils in innate host defense against *Staphylococcus aureus* infections.

Semin Immunopathol 2012; 34(2): 237–259. doi: 10.1007/s00281-011-0295-3.

31. Wang BS, Huang GJ, Tai HM*, et al.* Antioxidant and anti-inflammatory activities of aqueous extracts of *Schizonepeta tenuifolia* Briq. Food Chem Toxicol 2012; 50(3–4): 526–531. doi: 10.101 6/j.fct.2011.12.010.

32. Yang XN, Khan I, Kang SC. Chemical composition, mechanism of antibacterial action and antioxidant activity of leaf essential oil of *Forsythia koreana* deciduous shrub. Asian Pac J Trop Med 2015; 8(9): 694–700. doi: 10.1016/j.apj tm.2015.07.031.